Supplemental Information:

Low Energy Electron Attenuation Lengths in Core-Shell Nanoparticles

Michael I. Jacobs[1,2], Oleg Kostko[2], Musahid Ahmed,[2] Kevin R. Wilson[2,*]

[1]Department of Chemistry, University of California, Berkeley, CA 94720, United States

[2]Chemical Sciences Division, Lawrence Berkeley National Laboratory, Berkeley, CA 94720, United States

* Correspondence to: krwilson@lbl.gov, (510) 495-2474

BASEX reconstruction:

The BASEX algorithm used to extract kinetic energy spectra from the velocity map imaging (VMI) images reconstructs the 3D image by treating the projection and 3D image as a linear combination of the same basis set of functions and finding the expansion coefficients. This method requires cylindrical symmetry with respect to the polarization vector of the excitation laser.[1] Without cylindrical symmetry, the kinetic energy (KE) spectrum extracted from an image could be distorted. As can be seen in Figure 2, the photoemission images of KI and squalane nanoparticles at 11 eV are not symmetrical and one side of the particle is "shadowed." This arises when the absorption length of light is shorter than the radius of the nanoparticle and photoemission preferentially occurs from the side of the particle facing the light source.[2,3] However, cylindrical symmetry exists along the light propagation axis. Because light from the synchrotron is horizontally polarized, symmetry will still exist with respect to photoemission from the top/bottom and left/right halves of the nanoparticles (directions shown below in Figure S1a). To assess the potential for distortion from lack of cylindrical symmetry, we have simulated both symmetric

emission and non-symmetric emission using SIMION and extracted KE spectra from the resultant 2D VMI. In the first simulations, 10,000 electrons with 1, 2…, 10 eV KE are flown and mapped onto a detector. In the symmetric case, the emission angle is isotropic. As shown below in Figure S1a and S1b, in the non-symmetric case, the emission of electrons is constrained to a cone centered along the light propagation vector with a half angle of 45 degrees. This scenario represents an extreme situation where electrons can only be emitted from the front of the nanoparticle. It retains the top-bottom, left-right symmetry that exists in the nanoparticle photoemission, but lacks cylindrical symmetry with respect to the polarization vector of the light (i.e. extreme front-back asymmetry). The BASEX algorithm was used to reconstruct both the symmetric and non-symmetric simulations. As is shown below, the shapes of the extracted KE spectra are very similar (Figure S1c), with minimal distortions of the spectral features introduced by the emission asymmetry (Figure S1d). Because this level of symmetry is constant in all of the photoemission events, the KE spectra that are extracted with the BASEX algorithm can be used to calculate the electron attenuation lengths.

Furthermore, because the particles are ionized with single photon ionization and the coatings are much smaller than the radius of the particle, the asymmetry of the images does not change with changing coating thicknesses. This was assessed by calculating the asymmetry parameter which is equal to the ratio of image intensity in the shadowed half of the image to the intensity in the front half of the image.[2] The asymmetry parameters for experiments at 9, 10, and 12 eV photon energies are shown below in Figure S2. The asymmetry changes at different energies (due to different absorption lengths of light), but remains constant within each energy. Thus, while we do not expect the emission asymmetry to affect the resultant KE spectrum, the emission asymmetry remains roughly equal for all coating thicknesses.

Using the measured asymmetry parameters, a second set of simulations looking at broader distributions (more closely representing the experiment) of low energy photoelectrons were also performed. These simulations emitted 200,000 electrons with a Gaussian spread in kinetic energy centered at 1 eV (FWHM = 0.75 eV), 3 eV (FWHM = 1.5 eV), and 4 eV (FWHM = 2 eV). These energies were chosen to roughly match the experimental photoemission spectra (Figure 3). Similar symmetry conditions to those presented above were used, but the half angle of the cone was extended to 120 degrees. This angle was chosen because it resulted in images that had an asymmetry parameter of 0.5. This matches the smallest ~~experimental~~ asymmetry parameter (Figure S2) observed experimentally, and thus represents the most extreme~~,~~ case. ~~The BASEX algorithm was used to extract KE spectra from the simulated images.~~ As shown in Figure S3, the shapes of the spectra from the asymmetric and symmetric simulations are similar and match the expected input photoelectron distribution. In the asymmetric spectra, minor distortions are apparent only at very low KE. However, because only electrons with the highest KE are used to extract electron attenuation lengths, we do not expect these distortions to impact the electron attenuation lengths reported here.
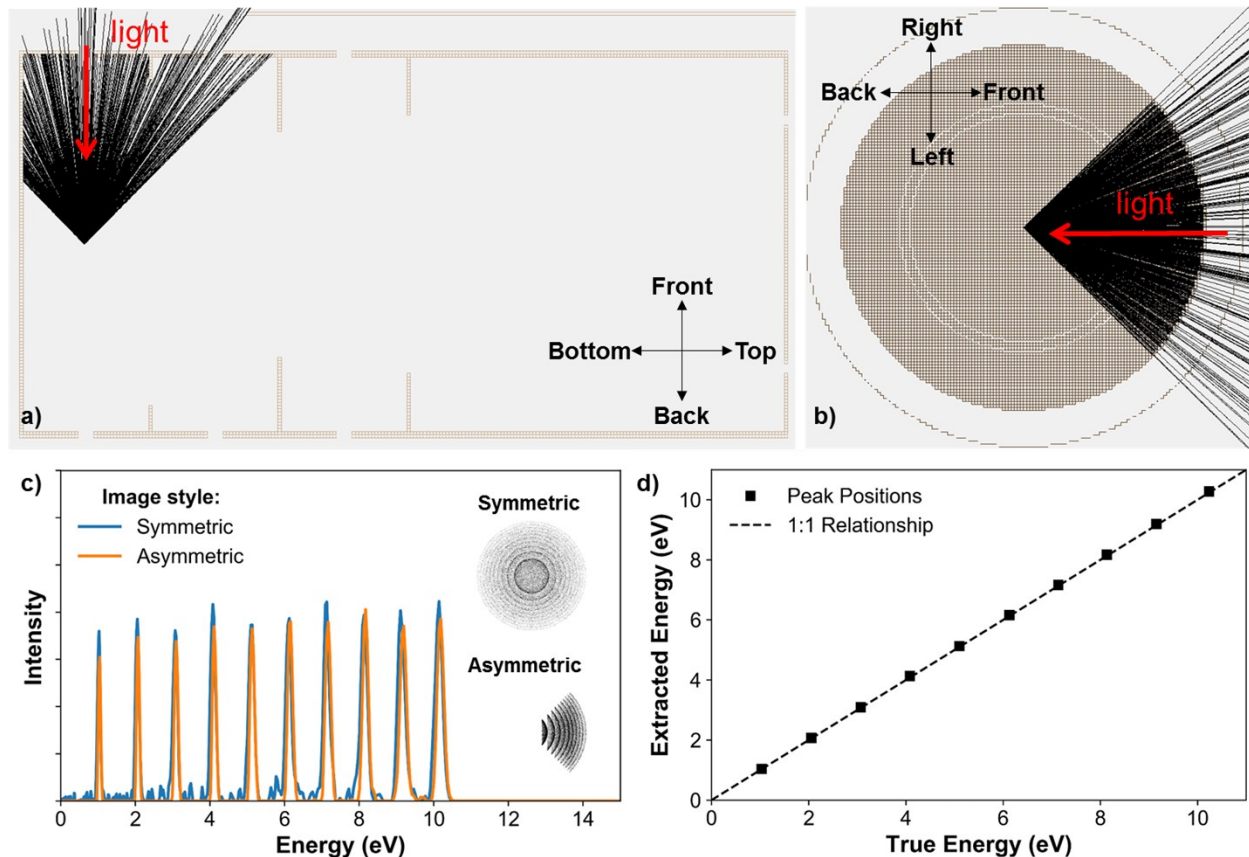
Figure S1. Cross-section of the VMI along drift tube (a) and down from detector (b) showing the modelled asymmetric ~~submission~~ of electrons. For the asymmetric emission, electrons are constrained to a cone centered along the light propagation vector with a half angle of 45 degrees. (Note: No electric fields are present in these images, and the trajectories of the electrons in these images do not match those when the simulation is run). c) The speed distribution of the symmetric simulated image (10,000 electrons with ~~10, 20... 100~~ eV kinetic energy emitted ~~randomly)~~ is compared with the speed distribution from an asymmetric simulated image. Both images pre-reconstruction are shown in the insets on the left. The speed distributions show that the overall shape of spectral features is unaffected by the asymmetry of the initial image. The asymmetric speed distribution is offset for clarity. d) The positions of the spectral features are compared to the "true" energies ascertained by the symmetric image. No radial distortion is present in the reconstruction from the asymmetric image.
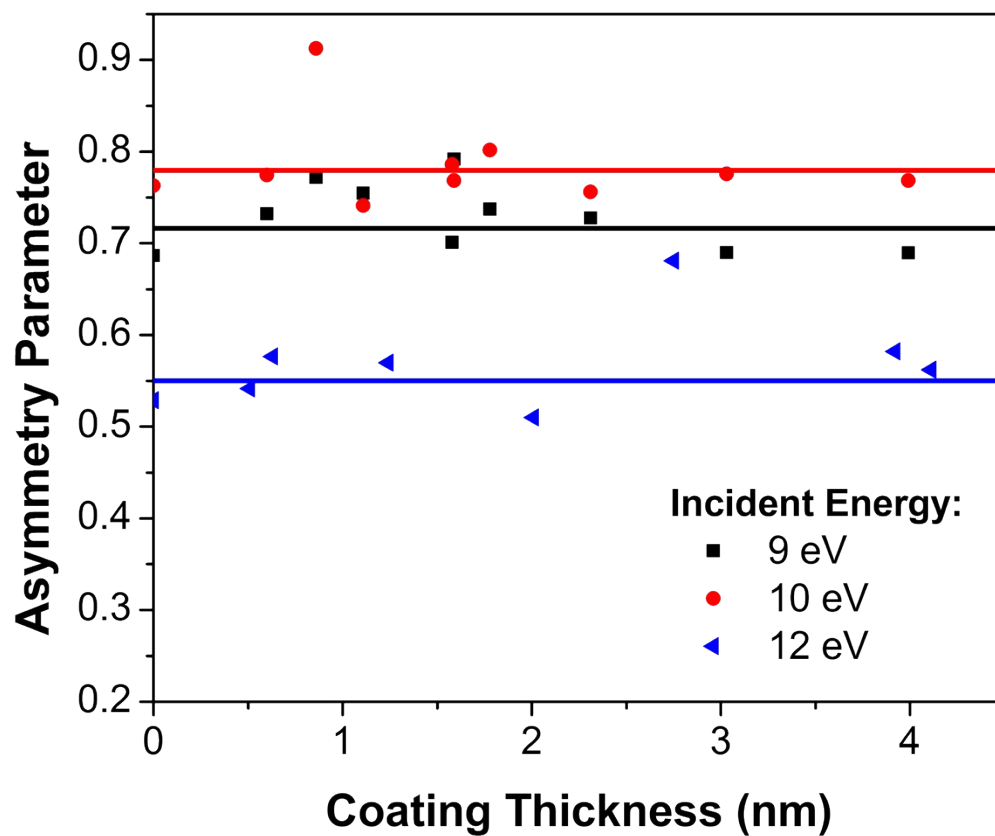
Figure S2. The asymmetry parameter for different 100 nm KI cores as a function of squalane coating thickness. At a given photon energy, the asymmetry parameter (i.e. the extent of shadowing) remains unchanged as the coating thickness increases.
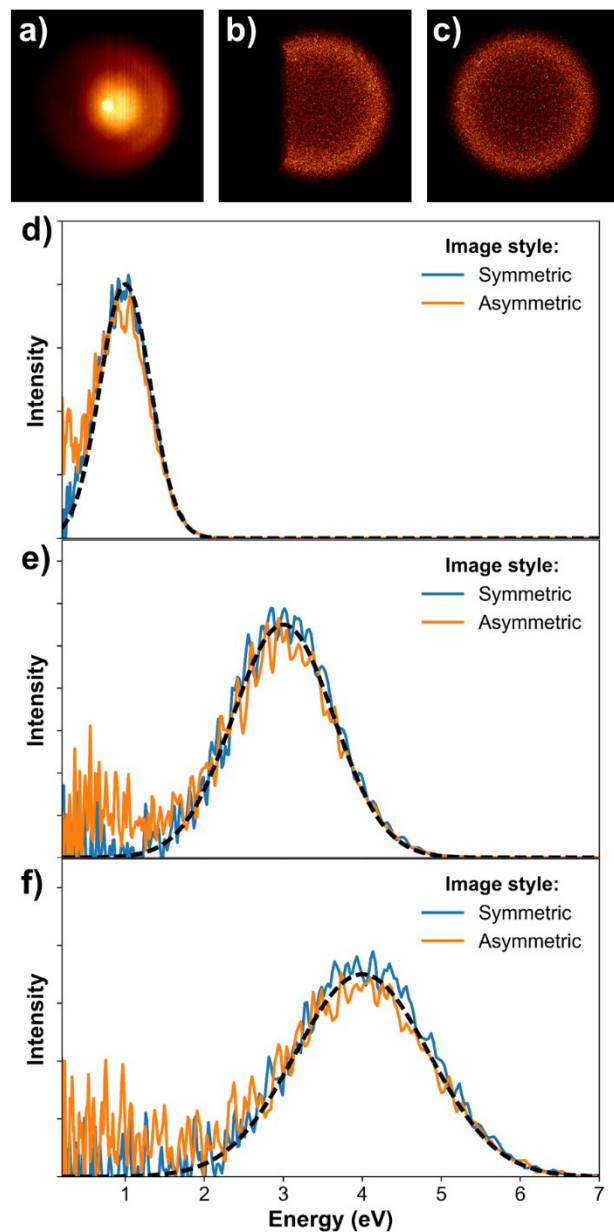
Figure S3. a) Example experimental photoemission image collected at 11 eV (from Figure 2). b) and c) Example simulated images that result from symmetric and asymmetric emission of electrons, respectively. The simulated asymmetric images (b) have an asymmetry parameter of 0.5 (i.e. two times as many electrons are collected on the right side of the image as compared to the left side). As shown in Figure S2, this resembles the most asymmetric image collected in this experiment. Kinetic energy spectra extracted from the simulated images with the BASEX algorithm are shown in d), e), and f). The emitted electrons in d), e), and f) have a Gaussian spread of kinetic energies centered 1 eV (FWHM = 0.75 eV), 3 eV (FWHM = 1.5 eV) and 4 eV (FWHM = 2 eV), respectively. The overall shapes of the reconstructed spectra match that of the input electron distribution (black dashed line). Minor distortions are only apparent at lower KE in the spectra from asymmetric emission.
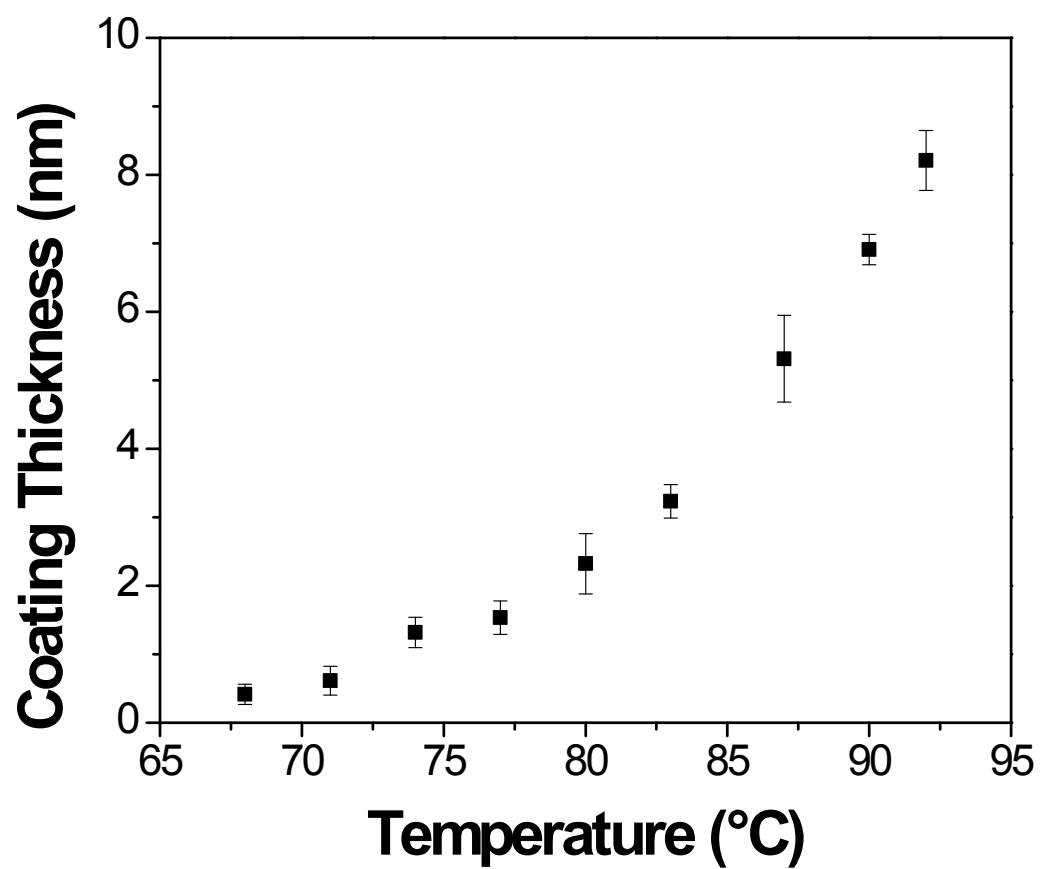
Figure S4. Squalane radial coating thickness vs. nucleation oven temperature.

Table S1. The real (n) and imaginary (κ) components of the refractive index of squalane at different photon energies. The imaginary component of the refractive index is used to calculate the probing depth of light (L_v). The values for n and κ are from Painter *et al.*[4]

Photon Energy (eV)	n	κ	L_v (nm)
8.5	1.90	0.33	35.2
9	1.89	0.40	27.5
10	1.80	0.55	18.9
11	1.68	0.70	12.8
12	1.50	0.82	10.0

Table S2. Comparison of EALs from different core shells. The size of the KI core was changed, which resulted in minimal differences in the measured EAL at 3.6 eV KE. Additionally, the core material was changed from KI to NaCl. This also did not result in a significant change in the measured attenuation length. Different photon energies were used to with the NaCl core compared to KI due to the difference in threshold energies (6.8 and 8.2 eV for KI and NaCl, respectively).[5]

Core Material	Photon Energy (eV)	KE (eV)	EAL (±1s) (nm)
100 nm KI	11	3.4±0.2	3.8±1.0
150 nm KI	11	3.4±0.2	5.5±1.3
200 nm KI	11	3.4±0.2	4.7±2.2
100 nm KI	9	2.1±0.2	4.4±2.1
100 nm NaCl	11	1.9±0.2	4.7±1.8

Table S3. The total electron yield (TEY) electron attenuation coefficients are calculated at the different photon energies. TEY measures the total electron intensity at each coating thickness. Because these measurements combine the decay from several different energies, the coefficients in Eq. 2 and Eq. 6 do not represent electron attenuation lengths, but rather average attenuation coefficients. Eq. 6 is used to calculate the average electron attenuation coefficient, L_{avg}. The TEY measurements from 12 eV are not reported due to large backgrounds at very low KE caused by higher harmonics from beamline 9.0.2.

Photon Energy (eV)	L_{avg} (nm)
8.5	18.8±5.1
9	4.9±1.8
10	4.4±1.0
11	7.0±3.7

References:

(1)   Dribinski, V.; Ossadtchi, A.; Mandelshtam, V. a.; Reisler, H. Reconstruction of Abel-transformable images: The Gaussian basis-set expansion Abel transform method. *Rev. Sci. Instrum.* **2002**, *73* (7), 2634 DOI: 10.1063/1.1482156.

(2)   Wilson, K. R.; Zou, S.; Shu, J.; Rühl, E.; Leone, S. R.; Schatz, G. C.; Ahmed, M. Size-dependent angular distributions of low-energy photoelectrons emitted from NaCl nanoparticles. *Nano Lett.* **2007**, *7* (7), 2014–2019 DOI: 10.1021/nl070834g.

(3)   Signorell, R.; Goldmann, M.; Yoder, B. L.; Bodi, A.; Chasovskikh, E.; Lang, L.; Luckhaus, D. Nanofocusing, shadowing, and electron mean free path in the photoemission from aerosol droplets. *Chem. Phys. Lett.* **2016**, *658*, 1–6 DOI: 10.1016/j.cplett.2016.05.046.

(4)   Painter, L. R.; Attrey, J. S.; Hubbell, H. H.; Birkhoff, R. D. Vacuum ultraviolet optical properties of squalane and squalene. *J. Appl. Phys.* **1984**, *55* (3), 756 DOI: 10.1063/1.333134.

(5)   Poole, R.; Jenkin, J.; Liesegang, J.; Leckey, R. Electronic band structure of the alkali halides. I. Experimental parameters. *Phys. Rev. B* **1975**, *11* (12), 5179–5189 DOI: 10.1103/PhysRevB.11.5179.